P1.16 VERTICAL PROFILES OF FREE RADICALS IN THE POLLUTED NOCTURNAL BOUNDARY LAYER: A ONE-DIMENSIONAL MODEL STUDY

Andreas Geyer*, Shuihui Wang, and Jochen Stutz
Department of Atmospheric Sciences, University of Los Angeles, Los Angeles

Abstract. The oxidation of anthropogenic and biogenic VOCs and NO_x in the polluted nighttime boundary layer (NBL) is primarily controlled by NO_3 radicals. NO_3 oxidation can also lead to the formation of secondary peroxy and even hydroxyl radicals. Calculations of the oxidation capacity of the NBL from in-situ or long-path measurements of NO_3 and other radicals are, however, very difficult because the assumption of a well mixed boundary layer is often not valid during night. Since VOCs and NO_x are emitted near the ground while NO_3 radicals are formed at all altitudes, we can expect unique vertical profiles of these species. Recent measurements and model studies show in fact pronounced vertical profiles of NO_3 in the NBL. Here we present results from a 1D chemical box model of the nocturnal radical chemistry. The model includes vertical transport based on measured micrometeorological data, deposition and emission, and a simplified NO_3 and RO_x chemistry module. The model reproduced vertical profiles of NO_3, NO_2, and O_3 observed near Houston, where up to 180 ppt NO_3 at the top of the NBL and 40 ppt at the ground were found. It was found that vertical transport cannot be neglected at night. At certain altitudes, vertical transport of NO_3 even is a more important NO_3 source than its chemical production. The results also show that steady state calculations so far used in the investigation of NO_3 and N_2O_5 chemistry are not representative in all cases. The model predicts high values of OH radicals close to the ground which are caused by downward transport of RO_2, formed by the reaction of NO_3 + VOCs in heights above 10 m, towards the ground, where RO_2 is converted into HO_2 and OH by the emissions of NO. The dependence of the nocturnal radical chemistry on vertical stability, NO, and VOC emission fluxes will be discussed.

1 INTRODUCTION

Nocturnal atmospheric chemistry and physics play a crucial role in the conversion and removal of air pollutants such as nitrogen oxides and VOCs. Because of missing solar radiation, trace gases follow different pathways (both chemically and physically) in the nocturnal boundary layer (NBL) than during day in the convective boundary layer (CBL). The convective conditions are suppressed by radiative cooling of the surface generating stable vertical stratification. Consequently, vertical turbulent transport produced by wind shear is often reduced by negative buoyancy [*Arya*, 1988; *Rao and Snodgrass*, 1979]. Trace gases emitted near the surface will therefore accumulate close to the ground leading directly and indirectly to strong vertical gradients of a number of species. Because of higher vertical stability during night, vertical transport is a key component determining the concentration levels and height profiles of many trace gases. Recently it became clear that vertical transport and chemical conversion cannot be separated from each other in the NBL [*Galmarini et al.*, 1997].

**Corresponding author address*: Andreas Geyer, University of California Los Angeles, Dept. of Atmospheric Sciences, 7127 Math Sciences Bldg., Los Angeles, CA 90095-1565;
Email: andreas@atmos.ucla.edu

Photolytic reactions, which are the driving force of atmospheric chemistry during daytime hours, are unimportant during night. As a consequence the free radical pool is modified: the NO_3 radical, which is rapidly photolysed during day (e.g., [*Magnotta and Johnston*, 1980; *Wayne et al.*, 1991]), replaces the OH radical, which is mainly produced by the photolysis of ozone, HONO, or aldehydes (e.g., [*Alicke et al.*, 2002; *Finlayson-Pitts and Pitts*, 2000]). Recently, however, first evidences were found that significant amounts of OH radicals could also be formed during night (e.g., [*Faloona et al.*, 2001; *Geyer et al.*, 2002]). The coupled effects of nocturnal boundary layer chemistry and limited vertical transport suggest unique vertical profiles of a number of species such as NO_3, NO_2, NO, O_3, and OH during nighttime.

Our present knowledge about the origin and development of height profiles of nocturnal key compounds such as NO_3, RO_2, HO_2, and OH is, however, very poor:

Recently, first evidence was found that NO_3 has an unique vertical profile in the NBL [*Aliwell and Jones*, 1998; *Fish et al.*, 1999; *Friedeburg et al.*, 2002; *Povey et al.*, 1998; *Weaver et al.*, 1996]. First reasonably resolved profiles of NO_3 above urban areas were measured by [*Friedeburg et al.*, 2002] and Wang et al. (P1.1, AMS2003) showing a strong increase of the NO_3 concentration up to the height of the NBL followed by a sudden decrease above the NBL. [*Friedeburg et al.*, 2002] found near ground values ($\approx$ 2 ppt) to be up to a factor 60 lower than at the top of the NBL, where 130 ppt were detected..

Height profiles of nocturnal RO_x radicals were not measured up to now. Although there are a number of RO_x models, e.g., [*Bey et al.*, 1997; *Bey et al.*, 2001; *Geyer et al.*, 2002; *Gölz et al.*, 2001; *Harrison et al.*, 1998], to our knowledge vertical transport was not considered in a nighttime RO_x model study so far.

In our poster, we present results from a 1D model to calculate vertical profiles of reactive traces gases (e.g., NO_3, O_3, RO_2, HO_2, OH) in the polluted nocturnal boundary layer. The model includes vertical transport, deposition and emission, and a simplified NO_3 and RO_x chemistry set. The origin of the NO_3 and RO_x profiles was investigated. The role of vertical transport for the vertical profiles of NO_3 and other reactive gases (especially RO_2, HO_2, OH) was quantified.

2 DESCRIPTION OF THE 1D - MODEL

The model is based on a system of one-dimensional transport-kinetics equations (eq. 1), where the rate of

change of the concentration $c(z, t)$ of a trace gas is expressed as the sum of the rate of change by vertical transport ($\frac{\partial}{\partial z}(\mathrm{Diff}(z)\cdot\frac{\partial c}{\partial z})$, based on Fick's second law), the rate of change by chemical reactions (total chemical production rate $P(z,t)$ and loss rate $L(z,t)$), and the emission rate $\Phi(z,t)$:

$$\frac{dc}{dt}=\frac{\partial}{\partial z}(\mathrm{Diff}(z)\cdot\frac{\partial c}{\partial z})+P(z,t)-L(z,t)+\Phi(z,t) \quad (1)$$

Concentration changes by advection are neglected in our model.

The model spans altitudes from the ground up to 100 m subdivided in 14 layers with a log-linear spacing between the layers. It includes an explicit calculation of the vertical exchange of all compounds between neighboring boxes, calculation of the temperature profile, a simplified chemical mechanism of nocturnal NO_x, NO_3, RO_x, O_3, and VOC chemistry, heterogeneous reactions on aerosols, emission of NO from the soil and cars, emission of monoterpenes from the biosphere, and dry deposition on the ground. Because the model is restricted to nighttime conditions, photolysis is not included. Key parameters of the model are its variable vertical mixing strength and the NO and VOC emission rates (as well as emission heights).

2.1 Vertical transport

The concentration change of a trace gas in a box by vertical exchange is calculated using Ficks' second law from the height depending sum of the laminar diffusion coefficient D, which is of the order of 0.1 cm^2/s, and the turbulent (eddy) diffusion coefficients $K(z)$. The calculation of the turbulent diffusion coefficient $K(z)$ is based on an interpolation formula suggested by [*Reichardt*, 1951]. $K(z)$ can reach values of several 10^4 cm^2/s:

$$K(z)=10^4\cdot\kappa\cdot u^*\cdot\frac{zi}{\Phi(\frac{z}{L})}(\frac{z}{zi}-\tanh(\frac{z}{zi})) \quad (cm^2/s), (2)$$

where κ is the von-Karman constant ≈ 0.4, u^* is the surface friction velocity, and z is the height above ground. Thereby, zi is an empiric constant (representing approximately the height, where laminar and turbulent diffusion are of the same value) given by [*Reichardt*, 1951] as $zi=10^{-5}\frac{\sqrt{T}}{u^*}$. The dimensionless correction function $\Phi(\frac{z}{L})$ is a function of the stability parameter, z/L, given by [*Businger et al.*, 1971] (with L being the Monin-Obukhow length).

Because a constant surface friction velocity is assumed the calculation of $K(z)$ is limited to the Prandtl layer covering approximately the first 50 - 100 m of the atmosphere.

The gradient of the potential temperature Θ in the Prandtl layer is calculated from the heat flux H according to an equation presented for example by [*Roedel*, 1992] as:

$$\frac{d\Theta}{dz}=-\frac{H}{c_p\cdot\rho}\cdot\frac{1}{\kappa\cdot u^*\cdot z}\Phi_H(\frac{z}{L}) \quad (3)$$

Here, c_p represents the heat capacity of the air, ρ its density, and $\Phi_H(\frac{z}{L})$ the dimensionless correction function for heat transport published by [*Businger et al.*, 1971]. The actual temperature profile, which can easily be derived from $\frac{d\Theta}{dz}$, is used in the calculation of temperature-dependent kinetic rate-constants within the chemical mechanism.

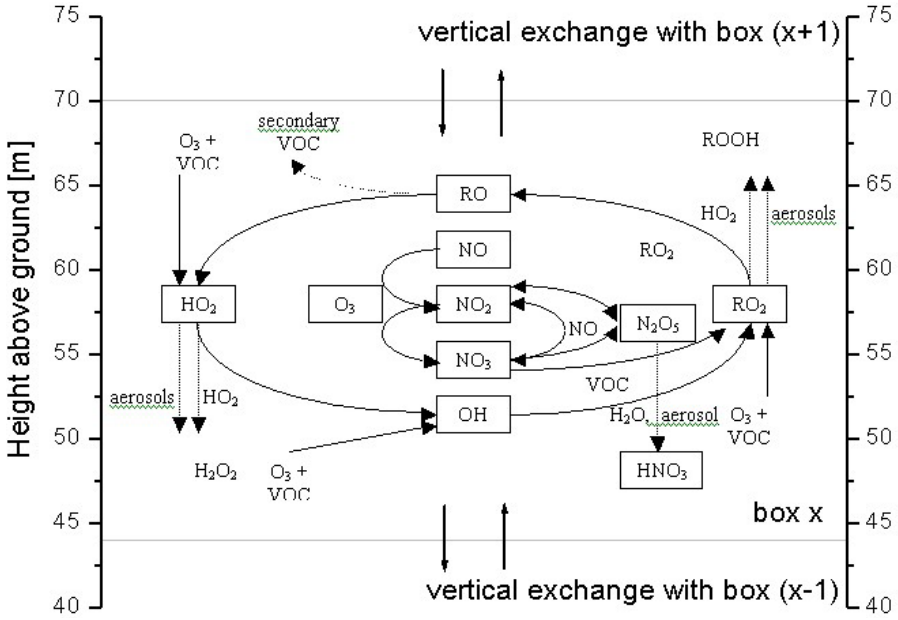

Figure 1. Chemistry and vertical transport of the 1D-boxmodel.

2.2 Chemical mechanism framework

The chemical reaction scheme of the model is shown in Figure 1. The inorganic reaction framework is taken from the Master Chemical Mechanism 3 (MCM3) published online under http://chmlin9.leeds.ac.uk/MCMframe.html. It is limited to three nocturnal key families: nitrogen oxides NO, NO_2, NO_3, N_2O_5, and HNO_3, ozone O_3, and the HO_x radical group OH and HO_2 (and the reservoir species HO_2NO_2) and reactions among each other. Updated rate constants are taken from [*DeMore et al.*, 1997; *Sander et al.*, 2000]. A key chain is the sequential oxidation of NO and NO_2 by O_3 into NO_3. The nitrate radical also reacts with NO back into NO_2. It also establishes a steady state with NO_2 and N_2O_5, which can react with water vapor or water adsorbed on aerosol surfaces. For this process an uptake coefficient of $\gamma(N_2O_5) = 0.05$ was chosen as suggested by the IUPAC subcommittee (June 2002)) for water droplets. Another reaction path of NO_3 is the reaction with unsaturated VOCs.

The oxidation mechanisms of three individual VOCs: α-pinene, isoprene, and propene are included in the model. The oxidation chains initiated by reactions with NO_3, OH, and O_3 generally follow the sequence VOC – RO_2 – RO – HO_2 – OH, which is discussed in detail by e.g., [*Geyer et al.*, 2002]. This sequence is carried by reactions of RO_2 and HO_2 with NO, NO_3, and RO_2. The alkoxy radical RO either reacts very fast with molecular oxygen to HO_2 or forms secondary VOCs by its thermal decay or isomerization. The self-reaction of HO_2 forms H_2O_2, which is an end product in the model. Peroxy radicals can also react on aerosol surfaces. Uptake coefficients of 0.01 and 0.015 were chosen for RO_2 and HO_2, respectively. In addition, ozonolysis can directly form HO_2 and OH radicals [*Paulson and Orlando*, 1996].

2.3 Deposition and emission

Dry deposition to the surface is calculated for reactive species in the lowest box, which is in contact with the ground. The number of molecules of each species in the this box colliding with the soil is calculated from kinetic gas theory and multiplied by the uptake coefficient γ to result in the loss on the ground. The following uptake coefficients were chosen:

$\gamma(O_3) = 0.002$, $\gamma(NO_2) = 0.0015$, $\gamma(NO_3) = 0.0005$, $\gamma(N_2O_5) = 0.05$, $\gamma(HNO_3) = 0.20$, $\gamma(RO_2) = 0.01$, $\gamma(HO_2) = 0.01$, and $\gamma(OH) = 0.005$.

These coefficients are based on the values suggested by the IUPAC subcommittee (June 2002)) for water droplets.

Nighttime emissions of NO and α-pinene are included in the model (see for example [*Fuentes et al.*, 2000; *Guenther et al.*, 2000] for more details about biogenic emissions). NO is emitted from the soil into the lowest box or by cars in 50 cm height. A homogeneous emission of α-pinene (for example from trees) was included between altitudes of 1 to 11 m.

2.4 Variation of input parameters

Height profiles were calculated for different scenarios, uncluding rural and urban environments, weak and strong atmospheric stability, and different temperatures (see Table 1).

3 Results

We discuss here first results of vertical profiles of O_3, NO_2, NO, NO_3, N_2O_5, and α-pinene for an urban case of high NO emissions at moderate vertical stability (typical urban situation, Run 20 from Table 1). Vertical profiles of RO_2, HO_2, and OH are discussed by Stutz et al. (4.2, AMS2003).

Figure 2 shows the vertical profiles of O_3, NO_2, NO, NO_3,

Run #	u* (m/s)	H (W/m^2)	T (K)	H_2O (cm^{-3})	p (mbar)	Aerosol surface ($\mu m^2/cm^3$)	NO_2 initial (ppb)	O_3 inital (ppb)	Isoprene initial (ppb)	Propene initial (ppb)	NO/α-pinene flux ($cm^{-2}s^{-1}$)
1	0.15	-7	290	2×10^{17}	1013	400	10	60	0.2	4	$10^{10}/3 \times 10^9$
2	**0.1**	**-15**	290	2×10^{17}	1013	400	10	60	0.2	4	$10^{10}/3 \times 10^9$
3	**0.25**	**0**	290	2×10^{17}	1013	400	10	60	0.2	4	$10^{10}/3 \times 10^9$
4	0.15	-7	**280**	2×10^{17}	1013	400	10	60	0.2	4	$10^{10}/3 \times 10^9$
5	0.15	-7	**300**	2×10^{17}	1013	400	10	60	0.2	4	$10^{10}/3 \times 10^9$
6	0.15	-7	290	2×10^{17}	1013	**100**	10	60	0.2	4	$10^{10}/3 \times 10^9$
7	0.15	-7	290	2×10^{17}	1013	**700**	10	60	0.2	4	$10^{10}/3 \times 10^9$
8	0.15	-7	290	2×10^{17}	1013	400	**1**	60	0.2	4	$10^{10}/3 \times 10^9$
9	0.15	-7	290	2×10^{17}	1013	400	**60**	60	0.2	4	$10^{10}/3 \times 10^9$
10	0.15	-7	290	2×10^{17}	1013	400	10	**10**	0.2	4	$10^{10}/3 \times 10^9$
11	0.15	-7	290	2×10^{17}	1013	400	10	**100**	0.2	4	$10^{10}/3 \times 10^9$
12	0.15	-7	290	2×10^{17}	1013	400	10	60	**0.05**	**0.4**	$10^{10}/3 \times 10^9$
13	0.15	-7	290	2×10^{17}	1013	400	10	60	**1**	**10**	$10^{10}/3 \times 10^9$
14	0.15	-7	290	2×10^{17}	1013	400	10	60	0.2	4	**$0/3 \times 10^9$**
15	0.15	-7	290	2×10^{17}	1013	400	10	60	0.2	4	**$10^{12}/3 \times 10^9$**
16	0.15	-7	290	2×10^{17}	1013	400	10	60	0.2	4	**$10^{10}/0$**
17	0.15	-7	290	2×10^{17}	1013	400	10	60	0.2	4	**$10^{10}/10^{11}$**
18	0.15	-7	290	2×10^{17}	1013	400	10	60	0.2	4	$10^{10} + 5 \times 10^{10} / 3 \times 10^9$
19	0.15	-7	290	2×10^{17}	1013	400	10	60	0.2	4	$10^{10} + 10^{11} / 3 \times 10^9$
20	0.15	-7	290	2×10^{17}	1013	400	10	60	0.2	4	$10^{10} + 5 \times 10^{11} / 3 \times 10^9$
21	**0.1**	**-15**	290	2×10^{17}	1013	400	10	60	0.2	4	$10^{10} + 5 \times 10^{10} / 3 \times 10^9$
22	**0.1**	**-15**	290	2×10^{17}	1013	400	10	60	0.2	4	$10^{10} + 10^{11} / 3 \times 10^9$
23	**0.1**	**-15**	290	2×10^{17}	1013	400	10	60	0.2	4	$10^{10} + 5 \times 10^{11} / 3 \times 10^9$

Table 1. Scenarios for 1D model.

N_2O_5, and α-pinene in the first 6 hours after model start. Throughout the night, NO, α-pinene, and NO_2 are increasing because of the NO and α-pinene emissions. As a consequence, O_3, NO_3, and N_2O_5 are decreasing. After 6h, O_3, NO_3, and N_2O_5 reached zero levels near the ground.

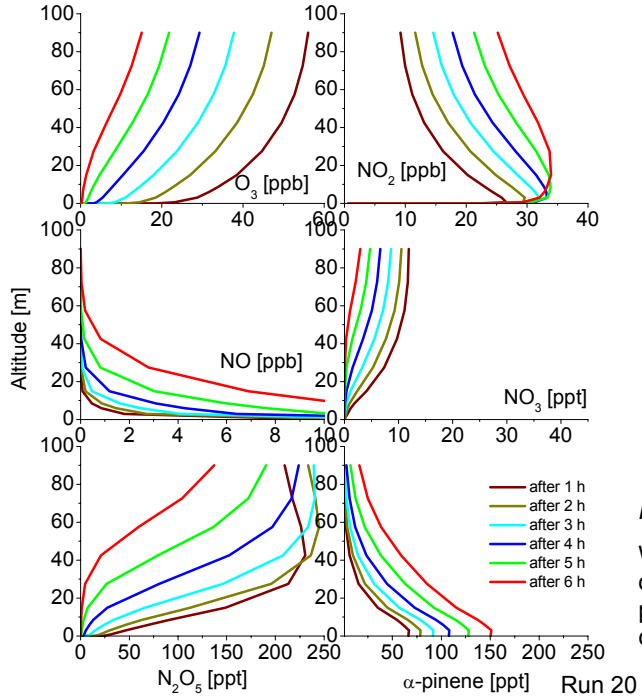

Figure 2. Vertical profiles of O_3, NO_2, NO, NO_3, N_2O_5, and α-pinene for urban scenario.

In short, the high NO emissions are the driving force for the chemistry of this scenario. Vertical mixing transports NO from the lowest 50 cm of the atmosphere to higher altitudes. In this scenario, NO reaches altitudes of 20 m after 1 h. In this NO enriched layer, NO reacts with O_3 to NO_2 resulting in a decrease of O_3 and an increase of NO_2 towards the ground. Vertical mixing transports a major part of the O_3 from altitudes above 20 m into the NO layer while NO_2 is transported out of this layer. This transport constitutes the main source of O_3 and the main sink of NO_2 below 20 m.

Vertical transport also plays a major role for the NO_3-N_2O_5 system (Figure 3): The chemical production rate of NO_3 is relatively constant with height. Its chemical sinks, however, are strongly depending on the altitude: The reaction with NO is the major sink of NO_3 below 15 m while loss of N_2O_5 on aerosols is the major (indirect) sink above this altitude. Reactions with VOCs or peroxy radicals play only a minor role in this scenario. Although direct vertical transport of NO_3 is negligible, a major part of N_2O_5 is transported from altitudes above 10 m towards the ground. There, its thermal decay forms about 25 - 50% of the NO_3 radicals (the path from N_2O_5 into NO_3 is favored because of the high loss frequency of NO_3).

Together, chemical processes and vertical transport result in a vertical profile of NO_3 with low, but not negligible, concentrations in the NO enriched surface layer (first 20 m) and higher but almost constant concentrations above this layer.

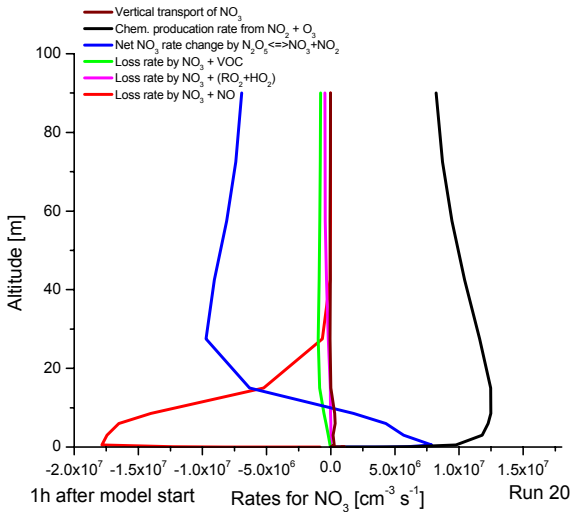

Figure 3. Rate analysis for NO_3 for urban scenario.

We can now quantify the contribution of vertical transport of NO_3 and N_2O_5 to the development of the NO_3 height profile. It was found in this study that the temporal change of N_2O_5 (dN_2O_5/dt) also has to be considered:

$$NO_3 = \frac{k_1\, NO_2\, O_3 + NO_3'v - \frac{dNO_3}{dt} + \frac{k_{2-}(N_2O_5'v - \frac{dN_2O_5}{dt})}{k_{2-} + k_3 Y}}{(k_{2+} - \frac{k_{2-}\, k_{2+}}{k_{2-} + k_3\, Y})\, NO_2 + k_4\, X} \qquad (4)$$

The constants k_1 – k_4 represent the rate constants of the reactions NO_2+O_3, NO_3+NO_2↔N_2O_5, of the sum of other N_2O_5 sinks Y, and other NO_3 sinks X, respectively.

It is apparent from Figure 4 and 5 that vertical transport of N_2O_5 and temporal change dN_2O_5/dt must be considered to calculate correct NO_3 height profiles.

4 The temperature profile and its impact on the NO_3 vertical profile

Because of surface cooling during night, modeled temperatures are generally increasing with height. In the case of very stable atmospheric conditions, our model predicts temperature differences of up to 10 K in the nocturnal boundary layer.

This vertical temperature profile impacts the NO_3 vertical profile significantly. Because of the strong temperature dependence of the thermal decay of N_2O_5, loss of N_2O_5 becomes more and more insignificant for the NO_3 concentration at increasing temperatures [*Geyer and Platt*, 2002] and the NO_3 levels increase. Therefore, the NO_3/N_2O_5 steady state shifts, leading to increasing NO_3 concentrations with altitude as a consequence of the increasing temperatures.

According to our calculations, the increasing temperature is the main cause of the NO_3 vertical profile above altitudes of 20 m.

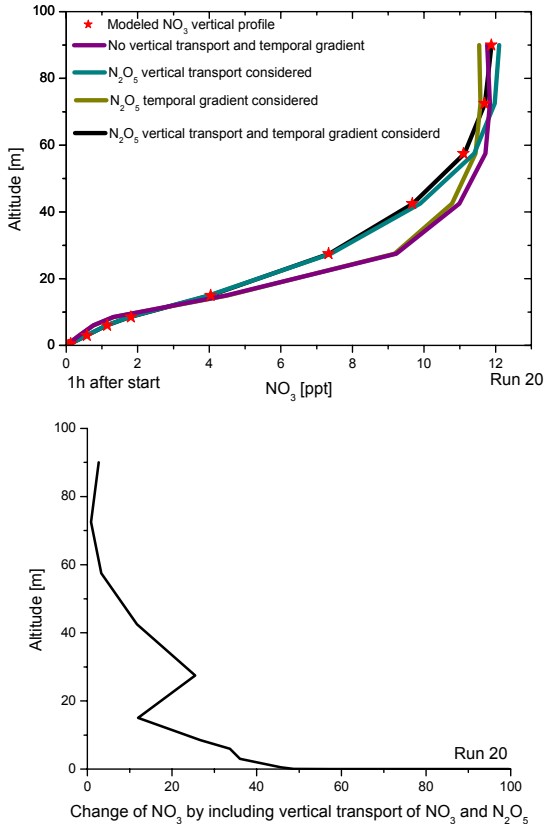

Figure 4 and 5. Contribution of vertical transport and temporal gradient of N_2O_5 to the development of the NO_3 height profile.

5 Conclusions

The following conclusions about the interaction of vertical transport and chemistry can be drawn from our model:

- The most important parameters determining the vertical distribution of all trace gases in the nocturnal boundary layer is the magnitude of vertical stability and the NO and VOC emissions.
- The model predicts NO_3 vertical profiles with increasing NO_3 with altitude. This is in agreement with measurements of the NO_3 profile (see Wang et al., P1.1, AMS2003).
- The vertical profile of NO_3 strongly depends on vertical transport and the temporal change of N_2O_5.
- The main reason for the NO_3 profile below 20 m are NO emissions from biosphere or traffic.
- The main cause for the NO_3 profile above 20 m is the temperature profile during nocturnal inversions.
- The model predicts clear vertical profiles of RO_2 and HO_2 with levels mostly increasing with height (see Stutz et al., 4.2, AMS2003).
- The Model predicts very high nocturnal OH concentrations of some 10^6 cm^{-3} in the first meter of the atmosphere (see Stutz et al., 4.2, AMS2003).

Literature:

Alicke, B., A. Geyer, A. Hofzumahaus, F. Holland, S. Konrad, H.-W. Pätz, J. Schäfer, J. Stutz, A. Volz-Thomas, and U. Platt, OH formation by HONO photolysis during the BERLIOZ experiment, *J. Geophys. Res.*, in press, 2002.

Aliwell, S.R., and R.L. Jones, Measurements of tropospheric NO_3 at midlatitude, *J. Geophys. Res.*, *103* (D5), 5719 - 5727, 1998.

Arya, S.P., *Introduction to Micrometeorology*, Academic Press, Inc., San Diego, 1988.

Bey, I., B. Aumont, and G. Toupance, The nighttime production of OH radicals in the continental troposphere, *Geophys. Res. Lett.*, *24* (9), 1067-70, 1997.

Bey, I., B. Aumont, and G. Toupance, A modelling study of the nighttime radical chemistry in the lower continental troposphere 2. Origin and evolution of HO_x, *J. Geophys. Res.*, *106* (D9), 9991 - 10001, 2001.

Businger, J.A., J.C. Wyngaard, Y. Izumi, and E.F. Bradley, Flux profile relationships in the atmospheric surface layer, *J. Atmos. Sci.*, *28*, 181-189, 1971.

DeMore, W.B., S.P. Sander, D.M. Golden, R.F. Hampson, M.J. Kurylo, C.J. Howard, A.R. Ravishankara, C.E. Colc, and M.J. Molina, Chemical kinetics and photochemical data for use in stratospheric modeling, JPL, Pasadena, 1997.

Faloona, I., D. Tan, W. Brune, J. Hurst, D. Barket, T.L. Couch, P. Shepson, E. Apel, D. Riemer, T. Thornberry, M.A. Carroll, S. Sillman, G.J. Keeler, J. Sagady, D. Hooper, and K. Paterson, Nighttime observations of anomalously high levels of hydroxyl radicals above a deciduous forest canopy, *J. Geophys. Res.*, *106* (D20), 24315-24333, 2001.

Finlayson-Pitts, B.J., and J.N. Pitts, *Chemistry of the upper and lower atmosphere: theory, experiments and applications*, xxii, 969 pp., Academic Press, San Diego, Calif. ; London, 2000.

Fish, D.J., D.E. Shallcross, and R.L. Jones, The vertical distribution of NO_3 in the atmospheric boundary layer, *Atmospheric environment*, *33* (5), 687 - 691, 1999.

Friedeburg, C., T. Wagner, A. Geyer, N. Kaiser, B. Vogel, H. Vogel, and U. Platt, Derivation of tropospheric NO_3 profiles using off-axis-DOAS measurements during sunrise and comparison with simulations, *J. Geophys. Res.*, *in press*, 2002.

Fuentes, J.D., M. Lerdau, R. Atkinson, D. Baldocchi, J.W. Bottenheim, P. Ciccioli, B. Lamb, C. Geron, L. Gu, A. Guenther, T.D. Sharkey, and W.R. Stockwell, Biogenic Hydrocarbons in the atmospheric boundary layer: A review, *Bulletin of the American Meteorological Society*, *81* (7), 1537 - 1575, 2000.

Galmarini, S., P.G. Duynkerke, and J. Vilà-Guerau de Arellano, Evolution of nitrogen oxide chemistry in the nocturnal boundary layer, *J. Appl. Meteo.*, *36* (7), 943 - 957, 1997.

Geyer, A., K. Bächmann, A. Hofzumahaus, F. Holland, S. Konrad, T. Klüpfel, H.W. Pätz, D. Perner, D. Mihelcic, H.J. Schäfer, A. Volz-Thomas, and U. Platt, Nighttime formation of peroxy and hydroxyl radicals during BERLIOZ - Observations and modeling studies, *J. Geophys. Res.*, in press, 2002.

Geyer, A., and U. Platt, The temperature dependence of the NO_3 degradation frequency - a new indicator forthe contribution of NO_3 to VOC oxidation and NO_x removal in the atmosphere, *J. Geophys. Res.*, doi: 10.1029/2001JD001215, 2002.

Gölz, C., J. Senzig, and U. Platt, NO_3-initiated oxidation of biogenic hydrocarbons, *Chemosphere - Global Change Science*, *3* (3), 339-352, 2001.

Guenther, A., C. Geron, T. Pierce, B. Lamb, P. Harley, and R. Fall, Natural emissions of non-methane volatile organic compounds, carbon monoxide, and oxides of nitrogen from North America, *Atmos. Environ.*, *34* (12-14), 2205-2230, 2000.

Harrison, R.M., J.P. Shi, and J.L. Grenfell, Novel nighttime free radical chemistry in severe nitrogen dioxide pollution episodes, *Atmos. Environ.*, *32* (16), 2769 - 2774, 1998.

Magnotta, F., and H.S. Johnston, Photodissociation quantum yields for the NO_3 free radical, *Geophys. Res. Lett.*, *7*, 769-772, 1980.

Paulson, S.E., and J.J. Orlando, The reactions of ozone with alkenes: an important source of HO_x in the boundary layer, *Geophys. Res. Lett.*, *23* (25), 3727-30, 1996.

Povey, I., A. South, A. Kint de Roodenbeke, C. Hill, R. Freshwater, and R. Jones, A broadband lidar for the measurement of tropospheric constituent profiles from the ground, *Journal of Geophysical Research*, *103* (D3), 3369 - 3380, 1998.

Rao, K.S., and H.F. Snodgrass, Some parametrizations of the nocturnal boundary layer, *Bound.-Layer Meteor.*, *17*, 15-28, 1979.

Reichardt, H., Vollstaendige Darstellung der turbulenten Geschwindigkeitsverteilung in glatten Leitungen, *Z. Angew. Math. Mech.*, *31*, 208-219, 1951.

Roedel, W., *Physik unserer Umwelt: Die Atmosphäre*, 457 pp., Springer Verlag, Berlin, 1992.

Sander, S.P., R.R. Friedl, W.B. DeMore, A.R. Ravishankara, D.M. Golden, C.E. Kolb, M.J. Kurylo, R.F. Hampson, R.E. Huie, M.J. Molina, and G.K. Moortgat, Chemical Kinetics and Photochemical Data for Use in Stratospheric Modeling, Supplement to Evaluation 12: Update of Key Reactions, Evaluation Number 13, JPL, Pasadena, CA, 2000.

Wayne, R.P., I. Barnes, P. Biggs, J.P. Burrows, C.E. Canosa-Mas, J. Hjorth, G. Le Bras, G. Moortgat, D. Perner, G. Poulet, G. Restelli, and H. Sidebottom, The nitrate radical: Physics, chemistry, and the atmosphere, *Atmos. Environ.*, *25A*, 1-203, 1991.

Weaver, A., S. Solomon, R.W. Sanders, K. Arpag, and J. Miller, H. L., Atmospheric NO_3 off-axis measurements at sunrise: Estimates of tropospheric NO_3 at 40°N, *J. Geophys. Res.*, *101* (D13), 18,605 - 18,612, 1996.